



ORIGINAL ARTICLE

Ultrasound assisted synthesis of starch-capped Cu₂O NPs towards the degradation of dye and its anti-lung carcinoma properties



Hualei Zhang^{a,b,c,d}, Wenjing Xu^e, Ping Wang^{a,b,c,d}, Litao Zhang^{f,*}

^a Department of Radiotherapy, Tianjin Medical University Cancer Institute and Hospital, Tianjin 300060, China

^b National Clinical Research Center for Cancer, Tianjin 300060, China

^c Key Laboratory of Cancer Prevention and Therapy, Tianjin 300060, China

^d Tianjin's Clinical Research Center for Cancer, Tianjin 300060, China

^e Graduate School, Tianjin University of Traditional Chinese Medicine, Tianjin 300070, China

^f Institute of Fundamental Research, Tianjin Academy of Traditional Chinese Medicine Affiliated Hospital, Tianjin 300120, China

Received 3 June 2022; accepted 8 July 2022

Available online 13 July 2022

KEYWORDS

Cu₂O nanoparticles;
Starch;
Methylene blue;
Human lung adenocarcinoma;
In vitro condition

Abstract A unique starch encapsulated Cu₂O nanoparticles were synthesized through a simple and 'green' route using ultrasonic irradiation. The polar functional groups on the starch (OH) facilitate the NP capping and stabilization. Structural features of the material were assessed over several advanced techniques like fourier transformed infra-red (FT-IR), UV-vis spectroscopy, scanning electron microscopy (SEM), energy-dispersive X-ray spectroscopy (EDS), energy dispersive X-ray analysis (EDX) elemental mapping, transmission electron microscopy (TEM), X-ray diffraction analysis (XRD), and inductively coupled plasma-atomic emission spectrometry (ICP-AES) analysis. It was catalytically explored in reducing an organic dye (Methylene blue - MB) in the presence of NaBH₄ at ambient conditions, being monitored in a UV-vis spectrophotometer. The nanocatalyst was recycled 11 times keeping consistency in its reactivity. Biologically, the nanocomposite exhibited excellent cytotoxicity against lung adenocarcinoma (PC-14, LC-2/ad and HLC-1) cell lines without affecting the normal (HUVEC) cell line. IC₅₀ values of the nanocomposite were found at 618, 56 and 379 against HLC-1, LC-2/ad, and PC-14 cell lines respectively and accordingly, PC-14 afforded the best adenocarcinoma activity.

© 2022 Published by Elsevier B.V. on behalf of King Saud University. This is an open access article under the CC BY-NC-ND license (<http://creativecommons.org/licenses/by-nc-nd/4.0/>).

* Corresponding author.

E-mail address: litaozhangtj@yeah.net (L. Zhang).

Peer review under responsibility of King Saud University.



1. Introduction

Social development and industrial growth have upgraded the human standard of living but alongside has increased the threat of ecological damage. The absence of basic awareness and insufficient regulations are responsible for damaging the ecological units (Chong et al., 2010; Zhao et al., 2019; Sadjadi et al., 2020). Especially, water pollution has reached such an alarming level that it is a severe threat to all living creatures. This is majorly because of the disposal of waste and garbage, harsh chemicals, heavy metals, drugs, dyes and pigments from industries into the natural water streams (Cermakova et al., 2017; Ayad et al., 2017; Hitam and Jalil, 2020; Wang and Wang, 2018). Organic dyes are categorically toxic chemicals that can even cause life at risk. They can disperse quite easily into water and the resulting colored media impedes access to sunlight. This however seriously affects the marine ecosystem (Lai et al., 2019; Najafinejad et al., 2018; Naseem et al., 2018). Hence, contamination of dyes into wastewater has raised significant concerns and encouraged many scientific groups to investigate suitable techniques for excluding these pollutants. Now, among the several means like adsorption, oxidation, photochemical reduction, electrochemical degradation, membrane filtration, coagulation and catalytic reduction (Kurtan et al., 2016; Ali et al., 2018; Veerakumar et al., 2018; Hao et al., 2019; Zhu et al., 2018), the decrease in dyestuffs involving nanocatalysts has been one of the most prospective, lucrative and sustainable methods converting the organic contaminants into benign derivatives (Yadav et al., 2021a; Vaya et al., 2022; Yadav et al., 2022; Yadav et al., 2021b; Nasrollahzadeh et al., 2018a; Adyani and Soleimani, 2019; Ganapuram et al., 2015; Veisi et al., 2017). Being encouraged by this and also carrying over our research on the development of biomolecule modified novel catalysts and applications (Tamoradi et al., 2019; Veisi et al., 2016; Veisi et al., 2019a; Veisi et al., 2018a; Mirfakhraei et al., 2018; Veisi et al., 2018b; Veisi et al., 2020; Hemmati et al., 2020a; Veisi et al., 2018c; Veisi et al., 2019b), we report the ultrasound assisted synthesis of Cu₂O NPs being stabilized over starch (Cu₂O/starch nanocomposites) and their potential application in the degradation of an organic dye (MB) using NaBH₄ as hydrogen donor. The experiment was monitored over UV-vis spectroscopy and the nanocomposite was found to produce outstanding results by reducing it in 1 min. In addition to chemical reactivity, we also investigated the bio-relevance of Cu₂O/starch nanocomposites in the anticancer activity of the human lungs. Among the numerous lung-related ailments, lung cancer is the deadliest and leading in causing death among all the malignancies (Thun et al., 2008; Taylor et al., 2007). This is due to its rapid growth and dismal treatment effect (Teng et al., 2020). General symptoms of this disease are tiredness, loss of weight, bleeding with cough, breathing anomaly, chest pain and dysphagia (Hecht, 2012). The typical and conventional treatment procedures followed in lung-cancer including chemotherapy and radiotherapy have confronted serious side effects and hence it needs urgent reformulations of those (Alsharairi, 2019; Stahl et al., 2013). Consequently, in the last few years there has been an incessant search for alternate medicines to treat lung cancer. Some biocompatible nanomaterials involving noble metal NPs have been reported by a few research groups as potential anticancer drug candidates (Varma, 2012; Wang et al., 2021; Ahmeda et al., 2020; Sun et al., 2020). This has prompted us to use the Cu₂O/starch nanocomposites to treat the lung cancer. In this assessment we investigated the cytotoxicity of our material against the frequently used cell lines i.e., HLC-1, LC-2/ad, and PC-14 cell lines, *in-vitro*. Notably, it exhibited significant outputs in those biological studies producing the best results with the PC-14 cell line.

2. Experimental

2.1. Materials

All the chemicals and solvents required for catalyst synthesis and its applications were purchased from Sigma Aldrich and used directly without further purifications.

2.2. Synthesis of Cu₂O/starch nanocomposites

30 mL of an aqueous solution of CuCl₂·2H₂O (10 mM) was added to 100 mL of an aqueous starch solution under ultrasonic conditions (50 kHz, 450 W) and left for 10 min at 60 °C. 3 % NaOH solution was added until pH 11.0 and sonication further at 60 °C for 2 hr. The formation of the Cu₂O NPs was justified by a change in color from blue to reddish-brown. The synthesized nanocomposite was isolated by centrifugation, washed thoroughly with deionized water and dried in air.

2.3. Catalytic reduction of methylene blue (MB) over Cu₂O/starch nanocomposites

A mixture of 10 mL aqueous MB solution (3.1×10^{-5} M), 2 mL NaBH₄ solution (5.3×10^{-3} M) and 0.002 g Cu₂O/starch nanocomposites was triturated at room temperature. The progression was monitored over a UV-vis absorption spectrophotometer. Kinetics of the reaction was also studied from the plot of absorbance vs time. After the end of the reaction, the catalyst was isolated by centrifugation and reused further.

2.4. Evaluation of the anti-cancer activity of Cu₂O/starch nanocomposites

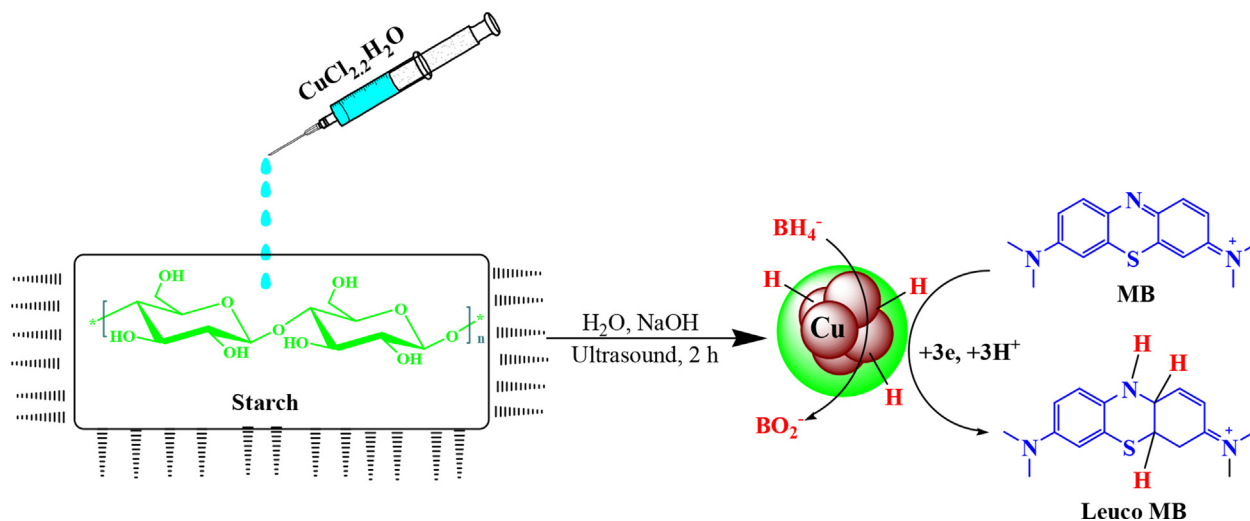
The typical MTT assay was used to evaluate the cytotoxicity of our material over the lung cancer cell lines, PC-14, LC-2/ad and HLC-1 and the normal cell line (HUVEC), which were prior cultured with Dulbecco's modified Eagle's medium (DMEM), and antibiotic media like penicillin and streptomycin. At first the cell lines went through incubation in 5 % CO₂ environment (37 °C, 24 hr) and then the catalyst samples with different concentrations (0–1000 µg/mL) were admixed. The cell wells were then incubated for 24 hr followed by sterilized for 2 hr in UV. Finally, MTT was introduced in all wells (5 mg/mL) and the corresponding absorbance was measured at 570 nm and % cell viabilities were estimated as

$$\text{Cell viability (\%)} = \frac{\text{Sample Ab.}}{\text{Standard Ab.}} \times 100$$

3. Results and discussion

3.1. Structural characterization of Cu₂O/starch nanocomposites

Scheme 1 depicts the schematic synthesis of Cu₂O/starch nanocomposites. The Cu₂O NPs were generated *in situ* from



Scheme 1 Ultrasound promoted synthesis of Cu₂O/starch nanocomposites under and the catalyzed reaction pathway for reducing MB.

Cu²⁺ ions over the starch bed in an alkaline medium being promoted by ultrasound irradiations. Starch molecules bearing the polar and electron-rich hydroxyl functions facilitate the binding, capping and stabilizing the tiny Cu₂O NPs. The biomolecular encapsulation also keeps the nanocomposite moieties from each other, thereby reducing the possibility of agglomeration. The as-synthesized material was analyzed using techniques such as UV–vis and FT-IR spectroscopy, FESEM, TEM, EDX and XRD. UV–vis spectroscopy was used to validate the presence of Cu₂O NPs. The corresponding plasmon resonance absorption band appears at ~472 nm (λ^{max}) and is shown in Fig. 1 (Maity et al., 2014).

FE-SEM and TEM analysis were used to determine the morphological properties of the recent nanocomposite (Figs. 2 and 3). Fig. 2 represents the FE-SEM images of the quasi-spherical Cu₂O/starch nanocomposites. Apparently, the particles look porous. The related outcomes also justify the SEM results. It reveals the perfectly spherical nanoparticles. The average diameter of the NPs was around 20 nm. The particles are observed to be well dispersed without any sign of aggregation.

To know the chemical constituent of Cu₂O/starch nanocomposites, EDX analysis was carried out and the profile

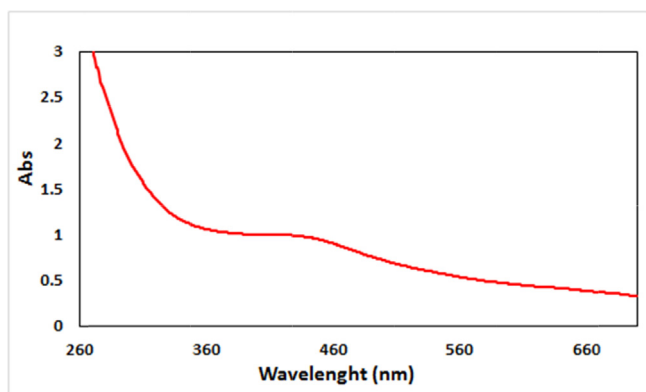


Fig. 1 UV–visible absorption spectra of Cu₂O/starch nanocomposites.

is shown in Fig. 4. The occurrence of Cu confirmed the successful synthesis of the nanocomposite. Au peaks come by default because of Au coating on the sample before the EDX analysis. The presence of C and O is strong evidence of biomolecular attachments (starch) thereby justifying the anticipated nanostructure. The results were further justified by the FE-SEM atomic mapping (Fig. 5). The compositional map reveals the C, O and Cu species to exist with excellent dispersion throughout the matrix surface.

Also, to verify the crystallinity and phase structure of the material, it was analyzed by XRD and the profile was compared to that of starch (Fig. 6). It exhibits a single phase XRD profile indicating it as a united moiety. The Bragg's peaks of starch are observed at 15.16°, 17.30°, 18.20°, 20.00° and 23.32°(2 θ) and match with literature reports (Castano et al., 2014; Yu et al., 2013). The XRD pattern of Cu₂O/starch nanocomposites displays the diffraction peaks at 2 θ = 77.23°, 73.48°, 61.39°, 42.39°, 36.48°, and 29.78° and are attributed to the reflections on (222), (311), (220), (200), (111), and (110) planes related to cubic Cu₂O NPs (JCPDS Card No. 05-0667) (Kuo and Huang, 2008).

Fig. 7 depicts the FT-IR spectra of Cu₂O/starch nanocomposites. FT-IR spectra shows the typical major vibrational peaks at 3421, 2924, 1602, 1382 and 1082 cm⁻¹ being attributed to overlapped phenolic O–H stretching, alkyl group C–H stretching, overlapped C–C stretching and O–H bending, C–H bending and C–O–C glycosidic linkage stretching vibrations respectively. It bears all the peaks of starch and finds close resemblances to Cu₂O NPs, validating the successful synthesis of desired material.

3.2. Cu₂O/starch nanocatalyzed reduction of MB

After the comprehensive analysis of the material, we aimed at the exploration of its catalytic competence in the degradation of MB using NaBH₄ as a reductant. UV–Visible spectrophotometer was used to screen the whole process. To the deep blue colored experimental solution of MB, the requisite amount of borohydride and catalyst was added. Alone NaBH₄ could not start the reaction without the catalyst. As soon as the

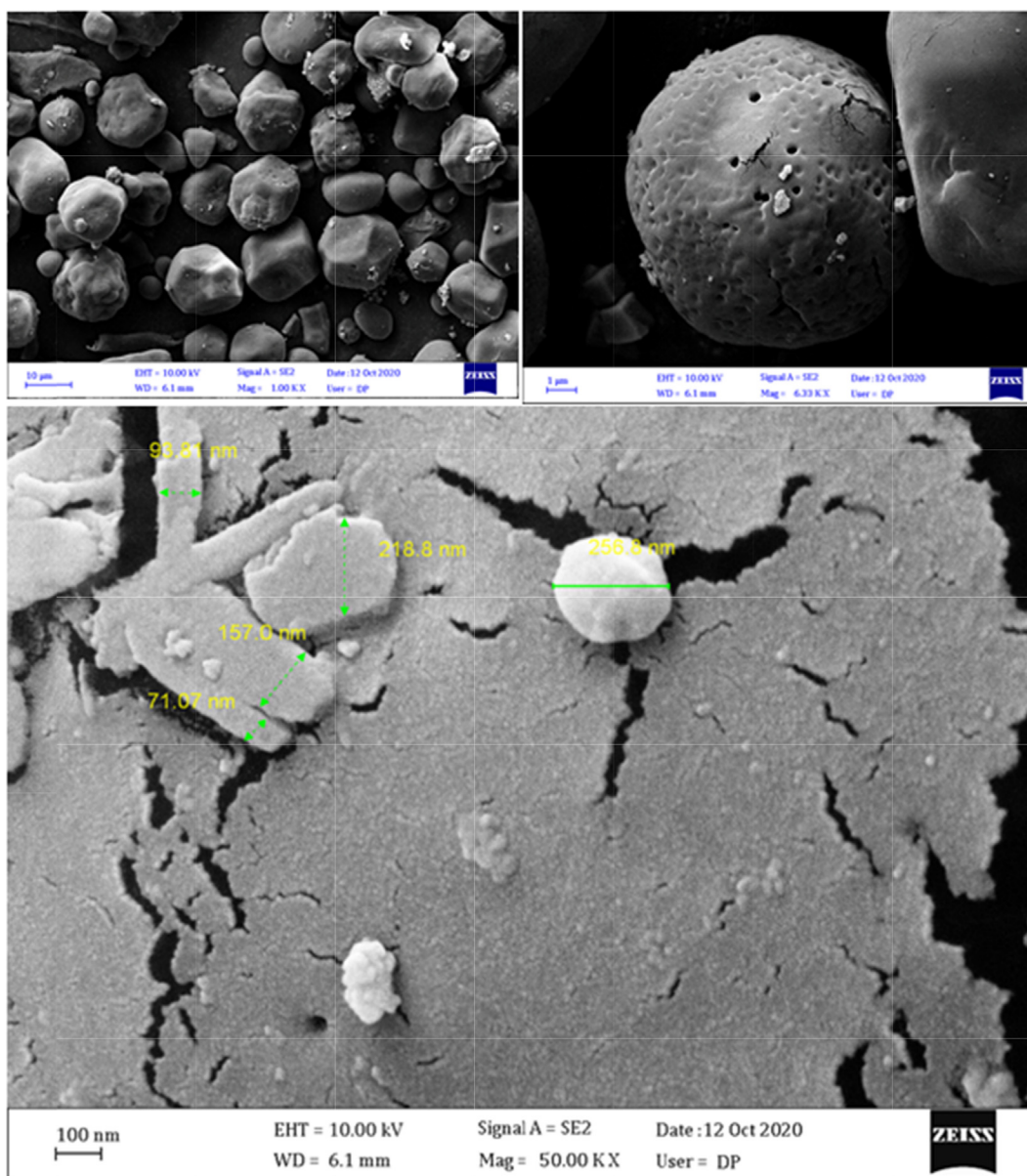


Fig. 2 FE-SEM images of Cu_2O /starch nanocomposites (scale bars are 10 μm , 1 μm and 100 nm).

degradation was initiated, the color of the experimental solution began fading out in no time. This could be quantitatively monitored with the decrease in absorption frequency (λ^{max}) of the experimental solution, being measured by the UV-vis spectrophotometer. A time-dependent absorbance plot showing the progress of the reaction has been displayed in Fig. 8a. As can be observed, the original absorption peak of 660 nm progressively decreased with time and became flattened within 60 s indicating the complete a reduction of MB towards the formation of Leuco MB. Following up with the data obtained, we studied the kinetics of the reaction by plotting $\ln(A_t/A_0)$ vs time. Since there occurs no change in the concentration of NaBH_4 , it can be concluded that the reaction follows pseudo-first-order kinetics. From the plot slope, the rate constant was estimated to be 0.056 s^{-1} using 2 mg of catalyst (Fig. 8b).

Regarding the mechanism, it is anticipated that the ultrasound energy activates the Cu_2O NPs by transferring electrons from its valence band to the conduction band. In this state, the hydride ions from NaBH_4 bind on the surface of the excited NPs. The high surface area, leading to high surface energy, also promotes this hydride binding. The activated or charged composite then transfers the electrons to the MB dye, which ultimately is reduced to Leuco MB.

3.3. Investigation of reusability and heterogeneity of Cu_2O /starch nanocomposites

In heterogeneous catalysis, the study of reusability is considered a fundamental criterion. Consequently, after completing a fresh catalyzed reaction over Cu_2O /starch nanocomposites, it was isolated by centrifuge, rinsed with EtOH and

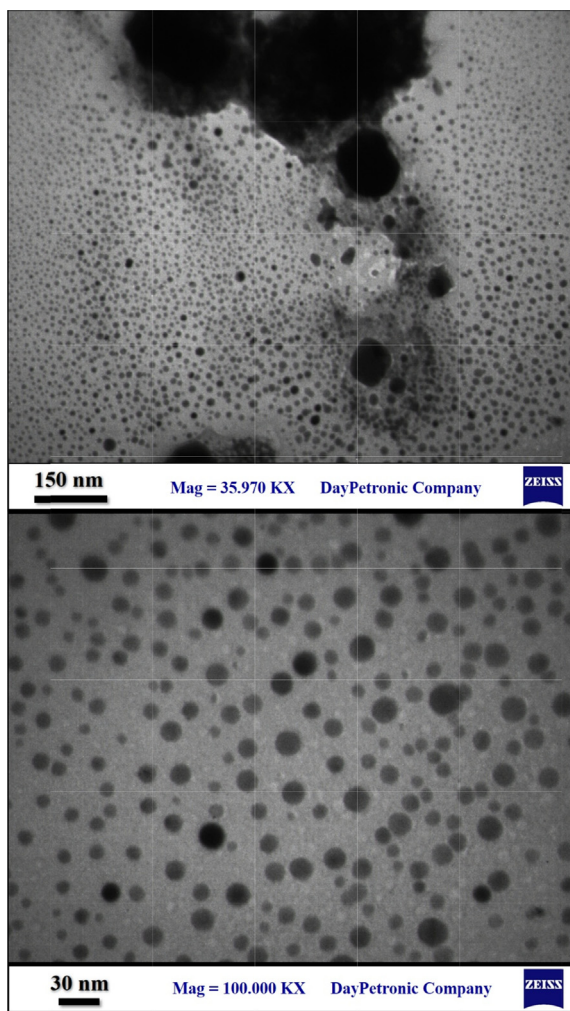


Fig. 3 TEM images of Cu₂O/starch nanocomposites.

regenerated by drying for the next runs. The study revealed that the Cu₂O/starch nanocomposites could be reused up to 11 consecutive runs with a nominal decrease in its activity and the profile is shown in Fig. 9a. Again, the heterogeneous nature of the catalyst and chances of leaching of Cu(I) species from the matrix were determined by a hot filtration test maintaining all conditions. During the mid-way a fresh reaction (35 s), the catalyst was isolated off when it was worth of 53 % conversion and the reaction filtrate was run for another 35 s keeping other conditions the same. Incidentally, there was no increment in the yield in the catalyst-free phase (Fig. 9b (ii)). This validates no leaching of active species from the nanocomposite and the Cu₂O/starch nanocomposites could be considered as a true heterogeneous catalyst. The fact was justified by the ICP-OES study of the reaction filtrate which disclosed that a very insignificant amount of Cu was leached out (0.01 wt%) and was also catalytically impotent.

3.4. Study of the reaction mechanism

Scheme 1 describes the plausible reaction pathway for reducing MB over Cu₂O/starch nanocomposites. Initially the incoming borohydride ions got adsorbed over Cu₂O NPs surface and

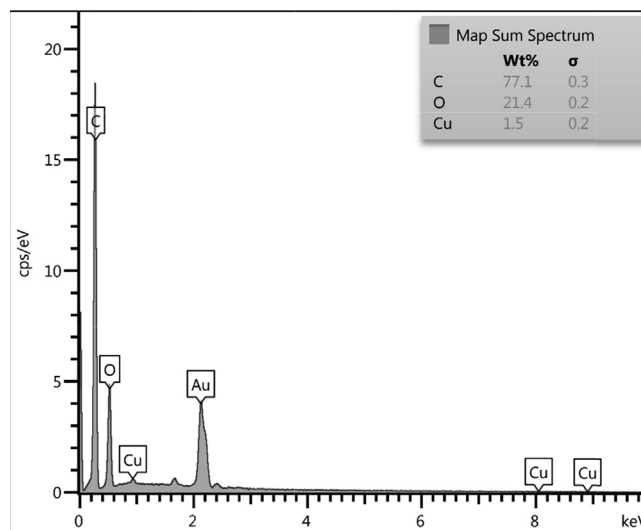


Fig. 4 EDX spectrum of the Cu₂O/starch nanocomposites.

released the H⁻ ion to form a Cu-hydride complex. MB is also simultaneously adsorbed onto the catalyst face. This is followed by the transmission of H⁻ ions to MB and generates Leuco MB. Thereafter, the reduced product leaves the surface and makes the site free for another cycle (Nasrollahzadeh et al., 2018b).

3.5. Exclusivity of catalytic results

Several reported protocols for the degradation of MB have been reviewed and compared with our results. The outcomes are documented in Table 1. It reveals that our devised protocol performs superior at ambient temperatures in terms of rate constants.

3.6. Investigation of bio-activity

After having an impressive catalytic result in the reductive degradation of MB dye, we focused on the bio-applications of Cu₂O/starch nanocomposites. Recently, the green synthesized biomolecular modified metallic nanocomposites have acquired noticeable significance in medicine, particularly, in exploring anti-cancer properties. Several studies have been conducted using noble metal nanocomposites (Varma, 2012; Wang et al., 2021; Ahmeda et al., 2020; Sun et al., 2020). Following the approach, we investigated the cytotoxicity of our material by studying its interaction with the three standard lung cancer cell lines along with the normal cell line for comparison through an MTT assay. The corresponding cell viabilities (%) were determined for different catalyst loads (0–1000 μ g/mL) and the consequences are demonstrated in Fig. 10. The cell viabilities decrease considerably with concentration for the first 3 cell lines unlike the HUVEC cell line. IC₅₀ values for the three cancer cell lines were 618, 566 and 379 μ g/mL respectively (Table 2), thus producing the best outcome with the PC-14 cell line.

Results of the bio-applications of our devised novel material (Cu₂O/starch nanocomposites) are very convincing

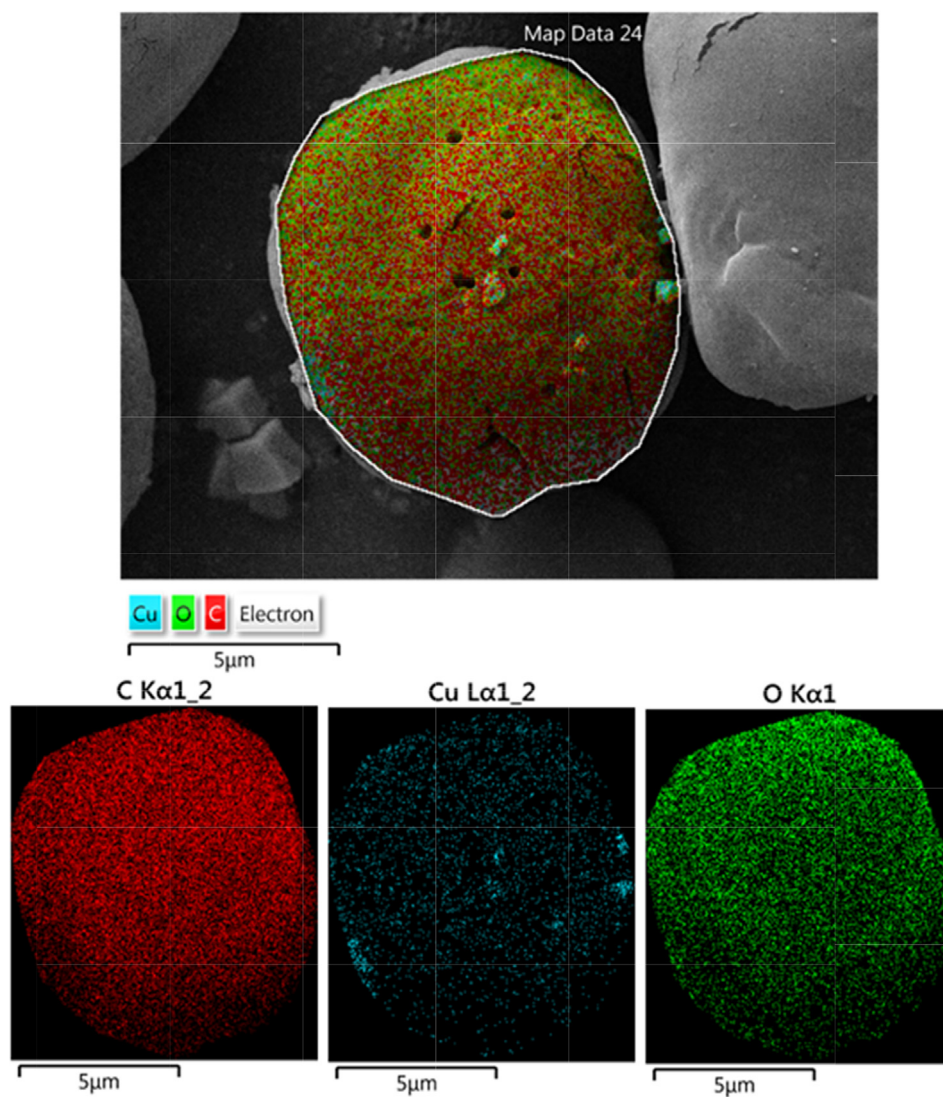


Fig. 5 FE-SEM image of biosynthesized Cu_2O NPs with its elemental mapping of Cu_2O /starch nanocomposites.

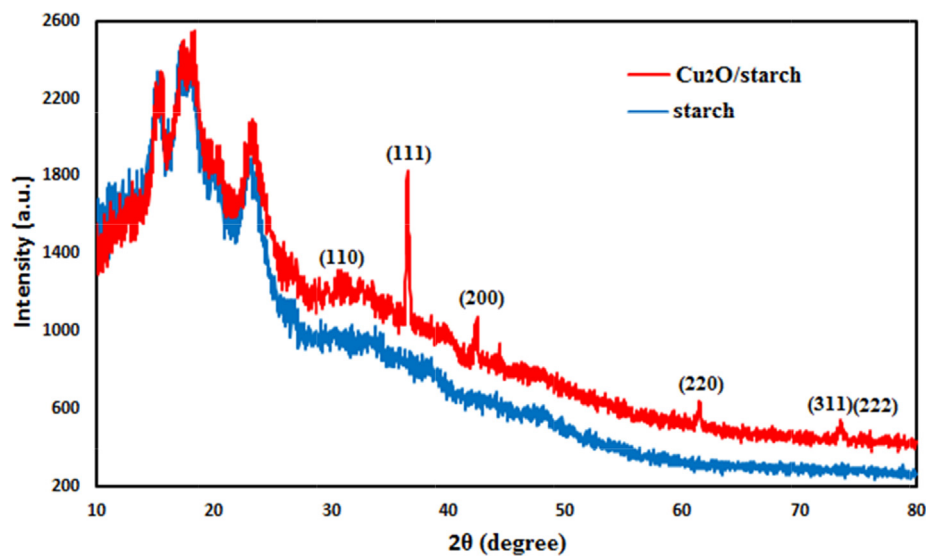


Fig. 6 X-ray diffraction study of Cu_2O /starch nanocomposites.

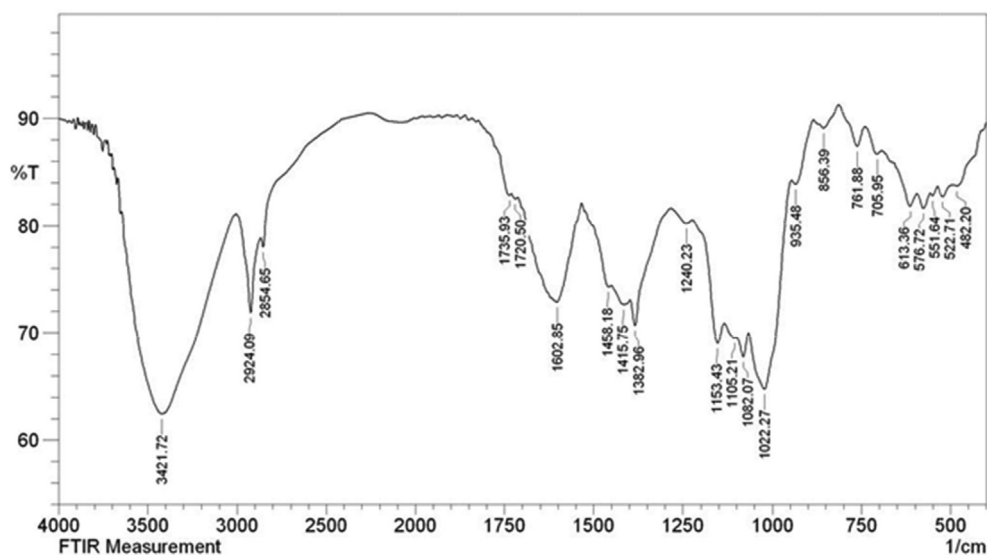


Fig. 7 The FT-IR spectrum of Cu₂O/starch nanocomposites.

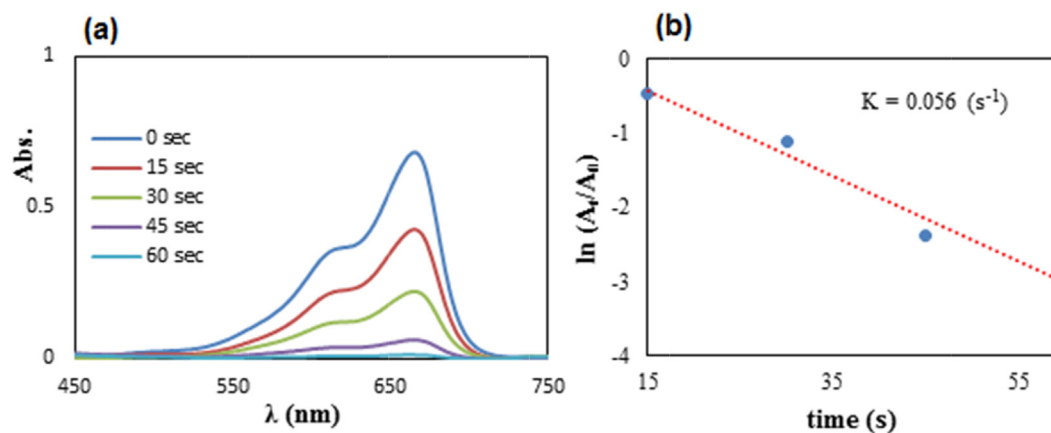


Fig. 8 (a) The spectrometric follow up in reducing MB using 2 mg of Cu₂O/starch nanocomposites, (b) The kinetic plot ($\ln A_t/A_0$ vs t).

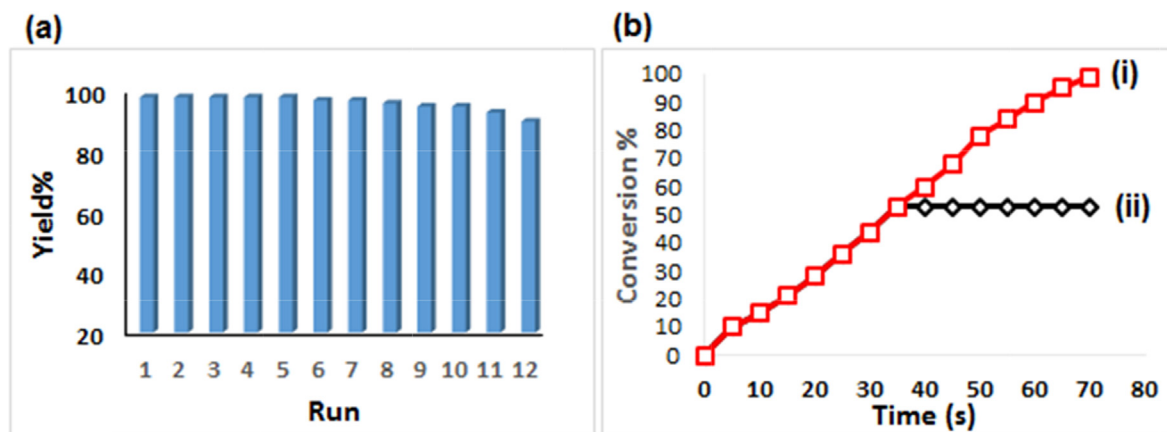


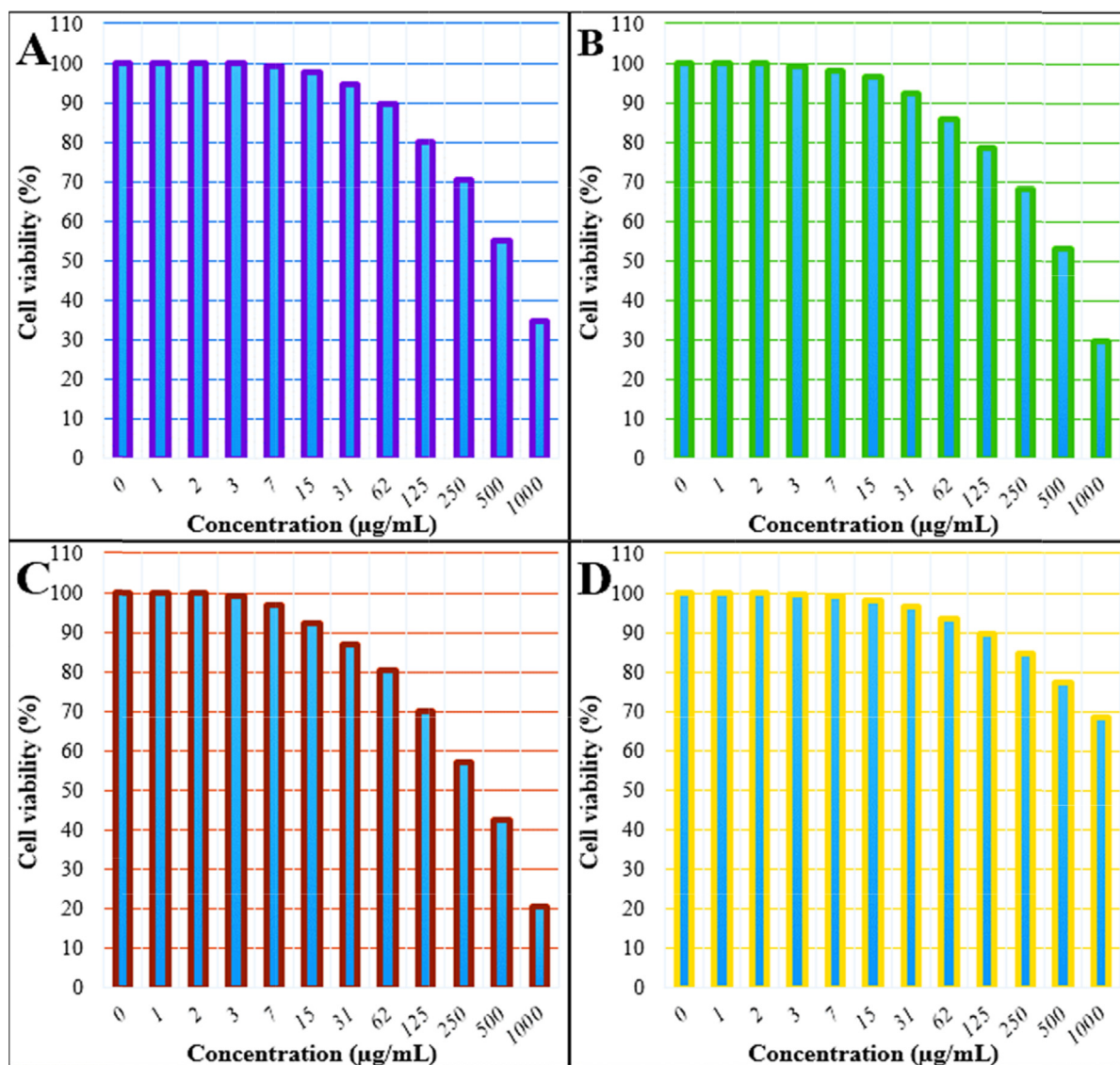
Fig. 9 (a) Reusability of Cu₂O/starch nanocomposites in reducing MB, and (b) Conversion % vs time (i) and the catalyst-free run (ii).

and could have a good prospect for alternative treatment for human lung cancer. The nature of biomolecular attachments, surface texture, particle shape, size and overall polarity of

the material play important role in overcoming the cell boundaries (Zangeneh and Zangeneh, 2020a; Zangeneh and Zangeneh, 2020b; Hemmati et al., 2020b; Zhaleh et al.,

Table 1 Comparison of the catalytic capacities of various catalysts reported in the literature for reducing MO by NaBH₄.

| Entry | Catalyst | T (K) | k (s ⁻¹) × 10 ⁻³ | Ref. |
|-------|---|-------|---|----------------------|
| 1 | MgAl-LDH@Au | 298 | 14 | (Kundu et al., 2003) |
| 2 | MgAlCe-LDH@Au | 298 | 30 | (Kundu et al., 2003) |
| 3 | Pd/Fe ₃ O ₄ @γ-AlOOH-YSMs | 298 | 51 | (Iqbal et al., 2017) |
| 4 | Fe ₃ O ₄ @Nico@Cu | 298 | 40 | (Cui et al., 2017) |
| 5 | CuO nanostructure | 308 | 11 | (Amir et al., 2015) |
| 9 | Cu ₂ O/starch | 298 | 56 | This work |

**Fig. 10** The Cell viability (%) of nanocomposite at different concentration against the cell lines HLC-1 (A), LC-2/ad (B), PC-14 (C), HUVEC (D).**Table 2** The IC₅₀ of nanocomposite with the different cell lines.

| | HLC-1 | LC-2/ad | PC-14 | HUVEC |
|--------------------------|-------|---------|-------|-------|
| IC ₅₀ (µg/mL) | 618 | 566 | 379 | – |

2019). A rapid augmentation of free radicals in normal cells drives the mutating of DNA and RNA structure which in turn proliferates the cancer cells. Hence, an anticipated good anticancer drug should have great antioxidant properties (Zangeneh et al., 2019a; Zangeneh et al., 2019b; Zangeneh et al., 2020; Zangeneh et al., 2019c; Mahdavi et al., 2019). We just focused on this concept to generate materials with

good anti-oxidant properties which could be very good at inhibiting the growth of lung cancer cells.

4. Conclusion

In summary, we have demonstrated a novel biopolymer functionalized nanomaterial by encapsulating starch over the *in situ* synthesized Cu₂O NPs, being promoted by ultrasound irradiations. Physicochemical characteristics of Cu₂O/starch nanocomposites were assessed through several analytical techniques. The mean size of the particles was around 20 nm, as determined by TEM analysis. The catalytic activity of the Cu₂O/starch nanocomposites was investigated in the reductive degradation of MB dye, a detrimental contaminant of water. UV-vis measurements confirmed the complete reduction of the dye in 60 min, being visibly confirmed from fading out of the existing blue color. The reaction followed pseudo-first-order kinetics with a considerably good rate constant. The material was so robust that it could be reused for successive 11 times without considerable leaching. Towards the bio-applications, it showed considerable prospect in controlling the proliferation of human lung cancer cells, being studied over three standard cancer cell lines (HLC-1, LC-2/ad and PC-14) and compared with normal cell line (HUVEC). In all the cases the % cell viability gradually decreased dose-dependently. Among the three cancer cell lines PC-14 exhibited the best inhibition over the nanomaterial, which has been manifested in the IC₅₀ values also. This validates that the starch-capped Cu₂O material could be a prospective alternate medicine in cancer therapeutics.

Declaration of Competing Interest

The authors declare that they have no known competing financial interests or personal relationships that could have appeared to influence the work reported in this paper.

References

Adyani, S.H., Soleimani, E., 2019. *Int. J. Hydrog. Energy* 44, 2711.

Ahmeda, A., Zangeneh, A., Zangeneh, M.M., 2020. *Appl. Organometal. Chem.* 34, e5290.

Ali, N., Awais, T., Kamal, M., Ul-Islam, A., Khan, S.J., Shah, A.Z.d., 2018. *Int. J. Biol. Macromol.* 111, 832.

Alsharairi, N.A., 2019. *Nutrients* 11, 725.

Amir, M., Kurtan, U., Baykal, A., 2015. *Chin. J. Catal.* 36 (2015), 1280–1286.

Ayad, M.M., Amer, W.A., Kotp, M.G., 2017. *Mol. Catal.* 439, 72.

Castano, J., Rodriguez-Llamazares, S., Contreras, K., Carrasco, C., Pozo, C., Bouza, R., Franco, C.M., Giraldo, D., 2014. *Carbohydr. Polym.* 112, 677–685.

Cermakova, L., Kopecka, I., Pivokonsky, M., et al, 2017. *Separ. Purif. Technol.* 173, 330e338.

Chong, M.N., Jin, B., Chow, C.W., et al, 2010. *Water Res.* 44, 2997e3027.

Cui, X., Zheng, Y., Tian, M., Dong, Z., 2017. *Appl. Surf. Sci.* 416, 103–111.

Ganapuram, B.R., Alle, M., Dadigala, R., Dasari, A., Maragoni, V., Guttena, V., 2015. *Int. Nano Lett.* 5, 215.

Hao, S.-M., Yu, M.-Y., Zhang, Y.-J., Abdelkrim, Y., Qu, J., 2019. *J. Colloid Interface Sci.* 545, 128.

Hecht, S.S., 2012. *Int. J. Cancer.* 131, 2724.

Hemmati, S., Joshani, Z., Zangeneh, A., Zangeneh, M.M., 2020a. *Appl. Organometal. Chem.* 34, e5267.

Hemmati, S., Heravi, M.M., Karmakar, B., Veisi, H., 2020b. *J. Mol. Liq.* 319, 114302.

Hitam, C.N.C., Jalil, A.A., 2020. *J. Environ. Manage.* 258, 110050.

Iqbal, K., Iqbal, A., Kirillov, A.M., Wang, B., Liu, W., Tang, Y., 2017. *J. Mater. Chem. A.* 5, 6716–6724.

Kundu, S., Ghosh, S.K., Mandal, M., Pal, T., 2003. *T. New J. Chem.* 27, 656–662.

Kuo, C.-H., Huang, M.H., o and Huang 2008. *J. Phys. Chem. C* 112, 18355–18360.

Kurtan, U., Amir, M., Baykal, A., 2016. *Appl. Surf. Sci.* 363, 66.

Lai, X., Guo, R., Xiao, H., Lan, J., Jiang, S., Cui, C., Ren, E., 2019. *J. Hazard Mater.* 371, 506.

Mahdavi, B., Paydarfard, S., Zangeneh, M.M., Goorani, S., Seydi, N., Zangeneh, A., 2019. *Appl. Organometal. Chem.* 33, e5248.

Maity, M., Pramanik, S.K., Pal, U., Banerji, B., 2014. *J. Nanopart. Res.* 16, 2179.

Mirfakhraei, S., Hekmati, M., HosseiniEshbala, F., Veisi, H., 2018. *New J. Chem.* 42, 1757.

Najafinejad, M.S., Mohammadi, P., Mehdi Afsahi, M., Sheibani, H., 2018. *J. Mol. Liq.* 262, 248.

Naseem, K., Farooqi, Z.H., Begum, R., Irfan, A., 2018. *J. Clean. Prod.* 187, 296.

Nasrollahzadeh, M., Issabaadi, Z., Sajadi, S.M., 2018a. *RSC Adv.* 8, 3723–3735.

Nasrollahzadeh, M., Mehdipour, E., Maryami, M., 2018b. *J. Mater. Sci.: Mater. Electron.* 29, 17054.

Sadjadi, S., Mohammadi, P., Heravi, M.M., 2020. *Sci. Rep.* 10, 6535.

Stahl, M. et al, 2013. *Ann.Oncol.* 24, 51.

Sun, T., Gao, J., Shi, H., Han, D., Zangeneh, M.M., Liu, N., et al, 2020. *Int. J. Biol. Macromol.* 165, 787.

Tamoradi, T., Veisi, H., Karmakar, B., 2019. *Chemistry Select* 4, 10953.

Taylor, R., Najafi, F., Dobson, A., 2007. *Int. J. Epidemiol.* 36, 1048.

Teng, L., Wang, K., Chen, W., Wang, Y.-S., Bi, L., 2020. *Pharmacol. Res.* 160, 105086.

Thun, M.J., Hannan, L.M., Adams-Campbell, L.L., 2008. *PLoS Med.* 5, e185.

Varma, R.S., 2012. *Curr. Opin. Chem. Eng.* 1, 123.

Vaya, D., Kaushik, B., Surolia, P.K., 2022. *Mater. Sci. Semicond. Process.* 137, 106181.

Veerakumar, P., PanneerMuthuselvam, I., Thanasekaran, P., Lin, K.-C., 2018. *Inorg. Chem. Front.* 5, 354.

Veisi, H., Taheri, S., Hemmati, S., 2016. *Green Chem.* 18, 6337.

Veisi, H., Azizi, S., Mohammadi, P., 2017. *J. Clean. Prod.* 70, 1536.

Veisi, H., Najafi, S., Hemmati, S., 2018a. *Int. J. Biol. Macromol.* 113, 186.

Veisi, H., Hemmati, S., Safarimehr, P., 2018b. *J. Catal.* 365, 204.

Veisi, H., Azizi, S., Mohammadi, P., 2018c. *J. Clean. Prod.* 170, 1536.

Veisi, H., Razeghi, S., Mohammadi, P., Hemmati, S., 2019a. *Mater. Sci. Eng. C* 97, 624.

Veisi, H., Tamoradi, T., Karmakar, B., Mohammadi, P., Hemmati, S., 2019b. *Mater. Sci. Eng. C* 104, 109919.

Veisi, H., Tamoradi, T., Rashtiani, A., Hemmati, S., Karmakar, B., 2020. *J. Indus. Eng. Chem.* 90, 379.

Wang, J., Wang, S., 2018. *Chem. Eng. J.* 334, 1502.

Wang, J., Wang, L., Cai, X., Karmakar, B., Zangeneh, M.M., Liu, H., 2021. *Mater. Chem. Phys.* 257, 123375.

Yadav, R., Chundawat, T.S., Rawat, P., Rao, G.K., Vaya, D., 2021a. *Bull Mater Sci* 44, 250.

Yadav, P., Surolia, P.K., Vaya, D., 2021b. *Materialstoday: Proceedings* 43, 2949–2953.

Yadav, P., Chundawat, T.S., Surolia, P.K., Vaya, D., 2022. *J. Phys. Chem. Solids* 165, 110691.

Yu, H., Cheng, L., Yin, J., Yan, S., Liu, K., Zhang, F., Xu, B., Li, L., 2013. *Food. Sci. Nutr.* 1 (4), 273–283.

Zangeneh, M.M., Bovandi, S., Gharehyakkeh, S., Zangeneh, A., Irani, P., 2019a. *Appl. Organometal. Chem.* 33, e4961.

Zangeneh, M.M., Zangeneh, A., 2020a. *Appl. Organometal. Chem.* 34, e5271.

- Zangeneh, M.M., Joshani, Z., Zangeneh, A., Miri, E., 2019b. *Appl. Organometal. Chem.* 33, e5016.
- Zangeneh, M.M., Zangeneh, A., Pirabbasi, E., Moradi, R., Almasi, M., 2019c. *Appl. Organometal. Chem.* 33, e5246.
- Zangeneh, A., Zangeneh, M.M., 2020b. *Appl. Organometal. Chem.* 34, e5290.
- Zangeneh, A., Zangeneh, M.M., Moradi, R., 2020. *Appl. Organometal. Chem.* 34, e5247.
- Zhaleh, M., Zangeneh, A., Goorani, S., Seydi, N., Zangeneh, M.M., Tahvilian, R., Pirabbasi, E., 2019. *Appl. Organometal. Chem.* 33, e5015.
- Zhao, W., Cao, B., Lin, Z., Su, X., 2019. *Environ. Pollut.* 254, 112961.
- Zhu, Z.-S., Qu, J., Hao, S.-M., Han, S., Jia, K.-L., Yu, Z.-Z., 2018. *ACS Appl. Mater. Interfaces* 10, 30.